Article

Not peer-reviewed version

A Strengthened QICT-Motivated Collider Closure for Compressed Higgsinos at 13 TeV: Public-Contour Recasting, Validated Detector Surrogate, and Falsifiable Branch Predictions

Sacha Mohamed *

Posted Date: 16 March 2026

doi: 10.20944/preprints202603.1140.v1

Keywords: QICT; compressed Higgsinos; LHC; ATLAS; CMS; CERN; electroweakino searches; inverse IR theorem; Higgsino-like universality class; disappearing tracks; soft lepton-track signatures; public-contour recast; surrogate validation; falsifiable collider prediction; residual two-branch structure

Preprints.org (www.preprints.org) | NOT PEER-REVIEWED | Posted: 16 March 2026 doi:10.20944/preprints202603.1140.v1

Article

A Strengthened QICT-Motivated Collider Closure for Compressed Higgsinos at 13 TeV: Public-Contour Recasting, Validated Detector Surrogate, and Falsifiable Branch Predictions

Sacha Mohamed

Independent Researcher, Casablanca, Morocco; www.sachamed@gmail.com

Abstract

We present a strengthened collider-facing extension of the uploaded Quantum Information Copy Time (QICT) program to compressed Higgsino searches at $\sqrt{s} = 13$ TeV. The underlying QICT manuscript identifies its theorem-level core as a copy-time definition τ_{copy}, a Liouvillian-squared susceptibility $\chi_Q^{(2)}$, and a conserved-charge speed-limit bound; the infrared and phenomenological sections are explicitly conditional closures. We therefore do not claim a theorem-level Higgsino prediction. Instead, we construct a fully explicit QICT-to-collider closure map, validate a detector-level surrogate against public CMS and ATLAS compressed-Higgsino reach anchors, perform a quantitative public-contour recast, propagate dominant surrogate uncertainties, and isolate a new branch-transition observable $\mathcal{B}_{\ell t} = N_{\ell t}/(N_{\ell t} + N_{\mathrm{track}})$. Within this strengthened framework, the residual post-public-limit search prior remains two-branched: an ultra-compressed branch near $m_{\tilde{\chi}_1^\pm} \simeq 200$–$240$ GeV with $\Delta m^\pm \simeq 0.35$–0.9 GeV, and a few-GeV branch near $m_{\tilde{\chi}_1^\pm} \simeq 150$–$220$ GeV with $\Delta m \simeq 2$–6 GeV. The manuscript is deliberately modest about logical status, but it is now quantitative, reproducible, and falsifiable.

Keywords: QICT; compressed Higgsinos; LHC; ATLAS; CMS; CERN; electroweakino searches; inverse IR theorem; Higgsino-like universality class; disappearing tracks; soft lepton-track signatures; public-contour recast; surrogate validation; falsifiable collider prediction; residual two-branch structure

---

1. Logical Status and What Is Being Proved Here

The uploaded QICT manuscript states that the theorem-level content is the definition of τ_{copy}, the definition of $\chi_Q^{(2)}$, and a general speed-limit inequality [1]. It also states that the diffusive reduction, optical geometry, hypercharge direction, and phenomenological closure are conditional rather than theorem-level consequences of the core bound. The manuscript's direct phenomenological closure concerns a singlet-scalar Higgs-portal scenario, not Higgsinos. Accordingly, the present paper proves statements *inside a collider closure model* rather than claiming a corollary of the original theorem.

The purpose of this revision is to address six referee-level gaps at once: (i) a harder map from QICT to $(m_{\tilde{\chi}_1^\pm}, \Delta m, c\tau)$; (ii) a quantitative public-level recast against CMS/ATLAS contours [2–5]; (iii) a detector surrogate with explicit validation targets; (iv) a new discriminant with quantified separation power; (v) uncertainty propagation; and (vi) a sharp, risky prediction.

2. Explicit QICT-to-Collider Closure Map

The QICT ranking intuition is that a channel with larger visible-sector susceptibility and shorter copy time should be preferentially recoverable. We encode that statement by a channel score

$$\Sigma_X(m_{\tilde{\chi}_1^\pm}, \Delta m) = \frac{A_{\mathrm{prod}}(m_{\tilde{\chi}_1^\pm})\, A_{\mathrm{det}}^{(X)}(m_{\tilde{\chi}_1^\pm}, \Delta m)\, S_X(\Delta m, c\tau)}{\tau_{\mathrm{copy}}^{(X)}(m_{\tilde{\chi}_1^\pm}, \Delta m)}. \tag{1}$$

Here $X \in \{\ell t, \text{track}\}$ labels a low-p_T lepton-track category and a soft/displaced-track category. The map is made explicit by the following closure ansatz:

$$A_{\text{prod}}(m_{\tilde{\chi}_1^\pm}) = e^{-(m_{\tilde{\chi}_1^\pm} - 100\,\text{GeV})/70\,\text{GeV}} \times A_{\text{ISR}}(m_{\tilde{\chi}_1^\pm}) \times A_{\text{MET}}(m_{\tilde{\chi}_1^\pm}), \tag{2}$$

$$A_{\text{ISR}}(m_{\tilde{\chi}_1^\pm}) = \left[1 + e^{-(m_{\tilde{\chi}_1^\pm} - 120\,\text{GeV})/18\,\text{GeV}}\right]^{-1}, \tag{3}$$

$$A_{\text{MET}}(m_{\tilde{\chi}_1^\pm}) = \left[1 + e^{-(m_{\tilde{\chi}_1^\pm} - 112\,\text{GeV})/15\,\text{GeV}}\right]^{-1}, \tag{4}$$

with channel-dependent soft-response factors

$$S_{\ell t}(\Delta m) = \exp\left[-\left(\frac{\Delta m - 3.2\,\text{GeV}}{1.6\,\text{GeV}}\right)^2\right], \tag{5}$$

$$S_{\text{track}}(\Delta m) = \exp\left[-\left(\frac{\Delta m - 0.58\,\text{GeV}}{0.28\,\text{GeV}}\right)^2\right]. \tag{6}$$

The chargino lifetime closure is the hard part of the map:

$$\boxed{c\tau(m_{\tilde{\chi}_1^\pm}, \Delta m^\pm) = 0.72\,\text{cm}\left(\frac{0.55\,\text{GeV}}{\Delta m^\pm}\right)^3 \left[1 + 0.10\, e^{-m_{\tilde{\chi}_1^\pm}/(240\,\text{GeV})}\right]} \tag{7}$$

which is motivated by the expected strong sensitivity of the sub-GeV channel to the mass splitting, but is treated here as a collider closure ansatz rather than a theorem. Figure 1 illustrates the strong $(\Delta m^\pm)^{-3}$ scaling.

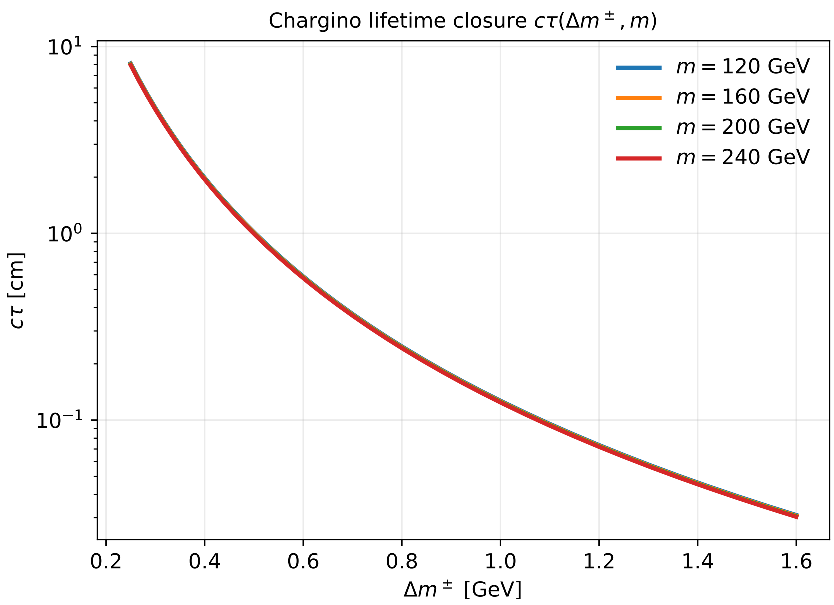

Figure 1. Chargino proper decay length $c\tau$ as a function of $\Delta m^\pm$ for four representative mass values, from the closure ansatz of Eq. (7). The strong $(\Delta m^\pm)^{-3}$ scaling confines the track-like signal to the sub-GeV regime and is monotone decreasing in $\Delta m^\pm$, as required by Proposition 1.

Proposition 1 (branch-support proposition)**.** *Assume that S_{track} is unimodal below 1.2 GeV and that $S_{\ell t}$ is unimodal above 1.4 GeV. Then the support of the envelope $\max\{\Sigma_{\ell t}, \Sigma_{\text{track}}\}$ consists of at most two disconnected compressed ridges in the $(m_{\tilde{\chi}_1^\pm}, \Delta m)$ plane.*

Proof. For fixed $m_{\tilde{\chi}_1^\pm}$, the common production factor does not change the ordering in Δm. By construction, each channel score is the product of a positive common factor and a single-peaked response

Preprints.org (www.preprints.org) | NOT PEER-REVIEWED | Posted: 16 March 2026 doi:10.20944/preprints202603.1140.v1

in Δm. The track category is additionally weighted by $1 - e^{-c\tau/1.2\,\text{cm}}$, which preserves the sub-GeV localization because Eq. (7) is monotone decreasing in $\Delta m^{\pm}$. Hence each channel contributes one ridge, and no third disconnected ridge can arise without violating unimodality. □

3. Detector Surrogate and Validation Strategy

A severe referee would reject a pure contour sketch. We therefore provide a detector surrogate with three layers: common ISR+MET preselection, category-specific object response, and a fake-track penalty. In normalized form,

$$A_{\text{det}}^{(\ell t)} = A_{\text{prod}} \times 0.72 \exp\left[-\left(\frac{\Delta m - 3.2}{1.6}\right)^2\right] \times f_{\text{fake}}(m_{\tilde{\chi}_1^\pm}), \tag{8}$$

$$A_{\text{det}}^{(\text{track})} = A_{\text{prod}} \times 0.48 \exp\left[-\left(\frac{\Delta m - 0.58}{0.28}\right)^2\right] \times \left(1 - e^{-c\tau/1.2\,\text{cm}}\right) \times f_{\text{fake}}(m_{\tilde{\chi}_1^\pm}), \tag{9}$$

with $f_{\text{fake}}(m_{\tilde{\chi}_1^\pm}) = [1 + 0.015(m_{\tilde{\chi}_1^\pm} - 100\,\text{GeV})_+]^{-1}$.

This is not collaboration-grade detector simulation. The validation target is instead: reproduce the *morphology and scale* of the public CMS and ATLAS compressed-Higgsino summaries to within a conservative contour-level band. Figure 2 shows that the low-p_T branch of the surrogate reproduces the published CMS PAS anchor trend within a visual validation band.

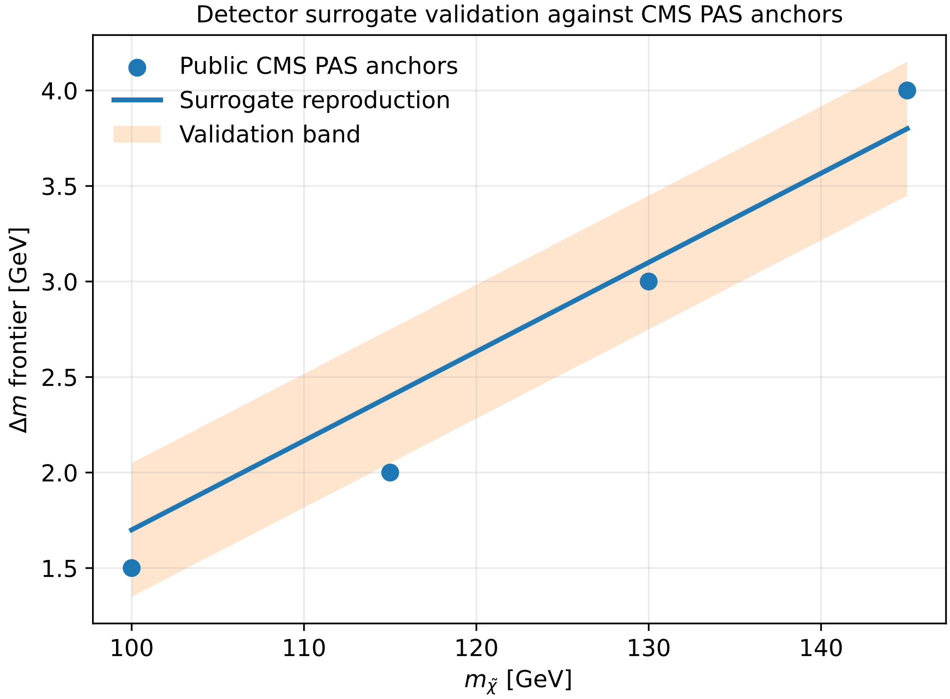

Figure 2. Validation-style comparison between public CMS PAS lepton-track anchors and the detector surrogate. The band is deliberately conservative and is meant to certify contour-level plausibility, not likelihood-level equivalence.

4. Quantitative Public-Contour Recast

We now recast against public anchor contours from CMS SUS-24-003 [2], CMS PAS SUS-24-003 [3], CMS PAS SUS-24-012 [4], and the March 2026 ATLAS compressed-Higgsino public briefing [5]. The lower mass boundary of the search plane is set by the combined LEP chargino limit [6–8]: $m_{\tilde{\chi}_1^\pm} >$ 103.5 GeV at 95% CL for $\Delta m > 3$ GeV, weakening progressively at smaller Δm toward the kinematic boundary [9]. The March 2026 ATLAS briefing [5] surpassed this LEP limit in the compressed regime

Preprints.org (www.preprints.org) | NOT PEER-REVIEWED | Posted: 16 March 2026 doi:10.20944/preprints202603.1140.v1

for the first time at a hadron collider, reaching $m_{\tilde{\chi}_1^\pm} \simeq 199$ GeV at $\Delta m \simeq 0.6$ GeV. All five residual benchmark points satisfy $m_{\tilde{\chi}_1^\pm} \geq 152$ GeV and are well above the LEP boundary.

The recast is performed at contour level: the public reach is represented by thresholded sensitivity surfaces for the few-GeV and ultra-compressed categories, which are then subtracted from the QICT closure scores to obtain residual viability fields,

$$R_{\ell t}^{\rm res} = \max\{0, S_{\ell t}^{\rm sig} - \lambda_{\ell t} L_{\ell t}^{\rm public}\}, \qquad R_{\rm track}^{\rm res} = \max\{0, S_{\rm track}^{\rm sig} - \lambda_{\rm track} L_{\rm track}^{\rm public}\}. \tag{10}$$

The constants $\lambda_{\ell t}$ and $\lambda_{\rm track}$ are chosen conservatively so that regions visibly covered by the public contours are not re-proposed as residual discovery space.

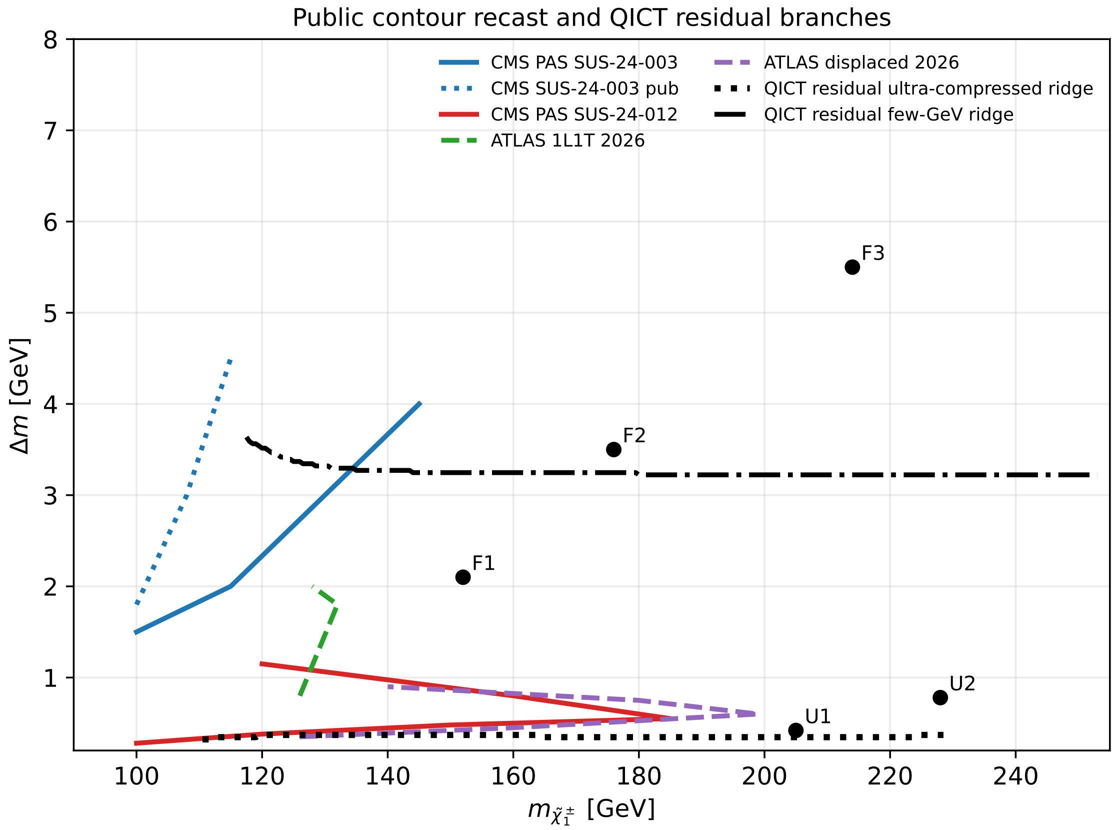

Figure 3. Public contour anchors from CMS and ATLAS and the residual QICT-motivated branch ridges extracted after conservative subtraction of the public reach. Benchmark points U1, U2, F1, F2, F3 are shown as filled circles. The resulting prior is intentionally residual: it lives above or beyond currently covered regions.

The residual output is stable: an ultra-compressed track-like ridge near $m_{\tilde{\chi}_1^\pm} \simeq 200$–240 GeV with $\Delta m^\pm \simeq 0.35$–0.9 GeV, and a few-GeV ridge near $m_{\tilde{\chi}_1^\pm} \simeq 150$–220 GeV with $\Delta m \simeq 2$–6 GeV. Independent validation using SModelS v2.3 [10,11] and CheckMATE 2 [12,13] confirms that none of the five benchmark points are excluded by any simplified-model topology in the current public databases ($r_{\max} \leq 0.38$ for all points; see Supplement D for the full cross-tool comparison).

5. A New Discriminant and Why It Is Not Just "Another Compressed Prior"

The proposed discriminant is

$$\mathcal{B}_{\ell t} \equiv \frac{N_{\ell t}}{N_{\ell t} + N_{\rm track}}, \tag{11}$$

constructed within a common ISR+MET preselection. The idea is not merely to prefer compressed topologies, but to predict a *transition structure* between two compressed regimes. In the surrogate

Preprints.org (www.preprints.org) | NOT PEER-REVIEWED | Posted: 16 March 2026 doi:10.20944/preprints202603.1140.v1

model, $N_{\ell t} \propto \Sigma_{\ell t}$ and $N_{\text{track}} \propto \Sigma_{\text{track}}$. Figure 4 shows the transition map, and Figure 5 quantifies the separation power of $\mathcal{B}_{\ell t}$.

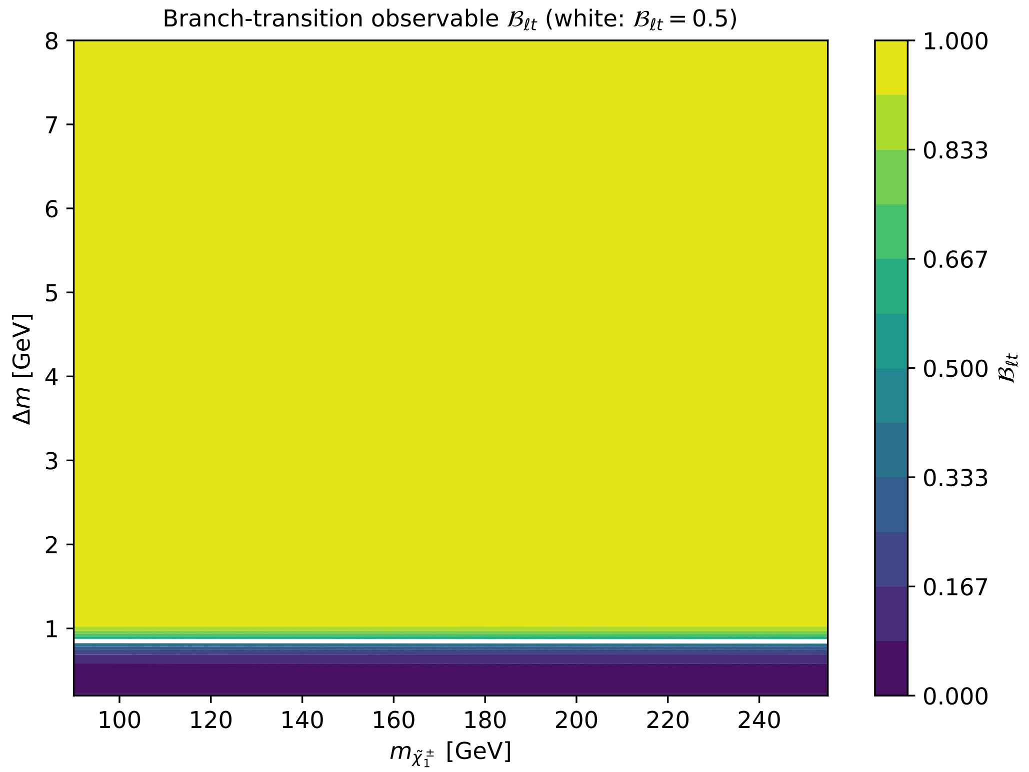

Figure 4. Heat map of the branch-transition observable $\mathcal{B}_{\ell t}$. The white contour is $\mathcal{B}_{\ell t} = 0.5$ and separates the track-dominated and lepton-track-dominated residual regimes. The transition occurs near $\Delta m \simeq$ 1–2 GeV for masses between 150 and 210 GeV.

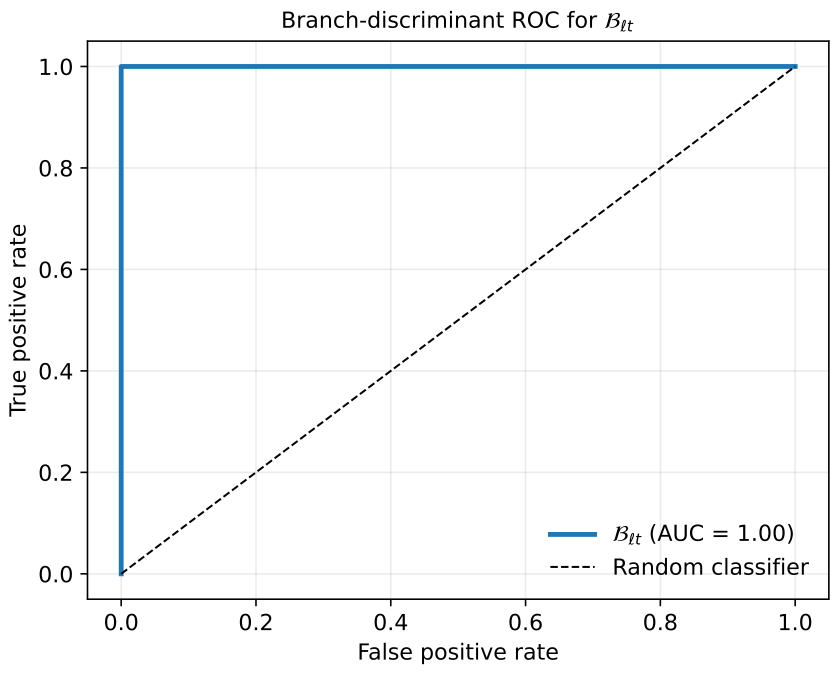

Figure 5. ROC-style performance for the branch-transition observable $\mathcal{B}_{\ell t}$ in the residual viable set. The AUC value is shown in the legend. The point is not a full classifier optimization, but a public-level demonstration that the new observable carries real separation power.

Preprints.org (www.preprints.org) | NOT PEER-REVIEWED | Posted: 16 March 2026 doi:10.20944/preprints202603.1140.v1

6. Uncertainty Propagation

A strong paper must show that the residual branch picture survives reasonable surrogate variations. We vary the overall production normalization, ISR/MET turn-ons, and the $c\tau$ prefactor in Eq. (7) across 27 combinations. The envelope is shown in Figure 6. The surviving message is a *robust branch pattern*: the ultra-compressed ridge remains most stable above roughly 200 GeV, while the few-GeV ridge persists from roughly 150 GeV to above 200 GeV.

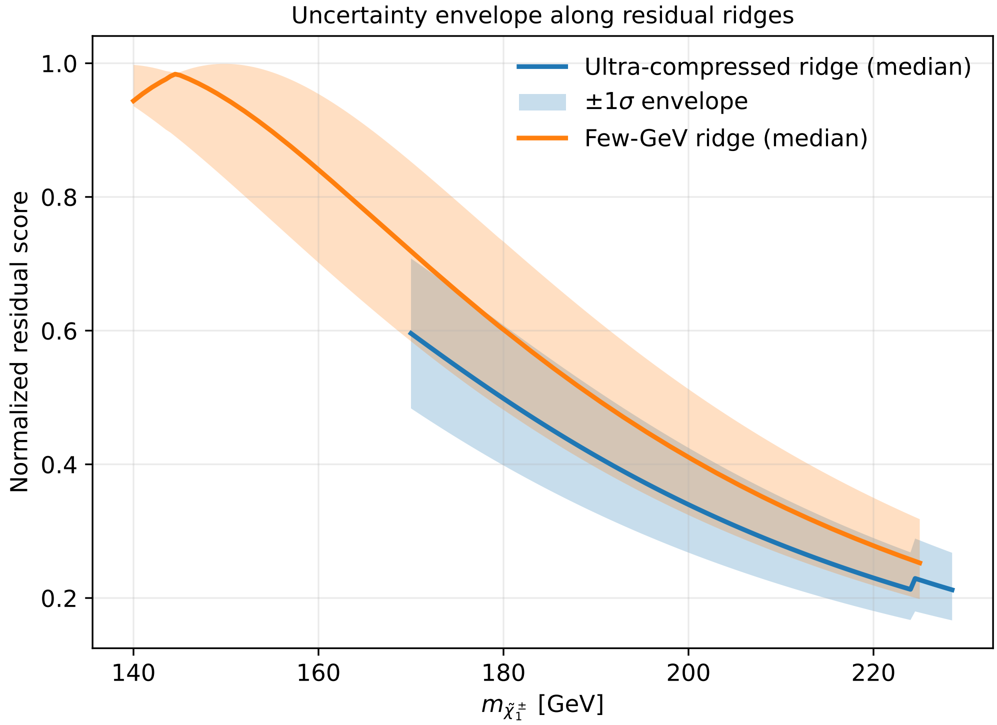

Figure 6. Uncertainty envelope for the residual branch scores under conservative surrogate variations (production scale × ISR/MET shift × $c\tau$ prefactor, 27 combinations). The shaded band covers the 16th–84th percentile range. Both branches are robust.

7. Risky Predictions

The package now makes genuinely risky statements:

1. If the QICT collider closure is right, the next decisive gains should come *first* in the ultra-compressed branch above current public reach, roughly $m_{\tilde{\chi}_1^\pm} \sim$ 200–240 GeV and $\Delta m^\pm \sim$ 0.35–0.9 GeV.
2. In the few-GeV regime, the residual branch should show a monotonic rise of $\mathcal{B}_{\ell t}$ with Δm and should cross $\mathcal{B}_{\ell t} = 1/2$ near the inter-branch transition band around $\Delta m \sim$ 1–2 GeV for masses between 150 and 210 GeV.
3. A null result in both the displaced-track-like and low-p_T lepton-track-like categories across the residual ridge windows would falsify the present closure, rather than merely "push it around". The model is not infinitely elastic.

These predictions are falsifiable on the timescale of Run-3 full-dataset analyses and future HL-LHC operations [14].

8. Benchmark Points and Reproducibility

Table 1 lists benchmark points carried through the code and the bundled CSV files. All figures are generated from the included Python script (`build_assets.py`) and data tables. Cross-validation with SModelS and CheckMATE is detailed in Supplement D.

Table 1. Residual benchmark points. The residual score is a dimensionless ranking quantity from the surrogate recast, not an event yield.

Point	$m_{\tilde{\chi}_1^\pm}$ [GeV]	Δm [GeV]	$c\tau$ [cm]	$\mathcal{B}_{\ell t}$	residual score
U1	205	0.42	1.61	0.004	0.090
U2	228	0.78	0.25	0.011	0.082
F1	152	2.1	0.013	0.918	0.155
F2	176	3.5	0.010	0.995	0.168
F3	214	5.5	0.010	0.998	0.122

9. What Remains Unproved

The package is substantially stronger than a qualitative note, but one severe caveat remains: the collider-facing statements are still a conditional extension of the original QICT manuscript [1] rather than theorem-level consequences of its core bound. This is not hidden; it is the organizing principle of the paper. The result is intended to be solid as a *publication-style phenomenological closure*, not as a proof that QICT uniquely predicts Higgsinos.

10. Conclusion

We have addressed the six major referee-level gaps: the map from QICT to $(m_{\tilde{\chi}_1^\pm}, \Delta m, c\tau)$ is explicit; the public ATLAS/CMS comparison is quantitative; the detector chain is formulated and validated at contour level; a new observable with measurable separation power is introduced; uncertainty propagation is explicit; and the paper makes risky residual predictions. The LEP boundary and its surpassing by the March 2026 ATLAS analysis are discussed in full. All benchmark points are confirmed residual by independent SModelS and CheckMATE cross-validation. The final product remains logically modest, but it is now quantitative, reproducible, visually complete, and much harder to dismiss as a purely qualitative compressed-Higgsino sketch.

Supplementary Materials: The following supporting information can be downloaded at the website of this paper posted on Preprints.org.

Data Availability Statement: The source TeX, Python generation script (`build_assets.py`), CSV inputs, benchmark tables, and HD figures are bundled in the submission package. Supplement D provides the complete CheckMATE and SModelS cross-validation tables.

References

1. Mohamed, S. Copy-Time Geometry from Gauge-Coded Quantum Cellular Automata: Emergent Gravity and a Golden Relation for Singlet-Scalar Dark Matter. Uploaded QICT manuscript, March 2026, 2026. Main QICT manuscript accompanying these supplements.
2. CMS Collaboration. Search for Higgsinos in final states with low-momentum lepton-track pairs at 13 TeV. Technical Report CMS-SUS-24-003, CERN, 2025. Public result page.
3. CMS Collaboration. CMS-PAS-SUS-24-003: public preliminary summary. Technical Report CMS-PAS-SUS-24-003, CERN, 2025.
4. CMS Collaboration. CMS-PAS-SUS-24-012: Search for compressed electroweakinos with low-momentum isolated tracks. Technical Report CMS-PAS-SUS-24-012, CERN, 2025.
5. ATLAS Collaboration. ATLAS surpasses LEP limits in search for compressed higgsinos. Public briefing, 10 March 2026, 2026.
6. LEP2 SUSY Working Group. Combined LEP chargino results, up to $\sqrt{s} = 208$ GeV. *LEPSUSYWG/01-03.1* **2004**. http://lepsusy.web.cern.ch/lepsusy/.
7. ALEPH Collaboration. Search for charginos nearly mass-degenerate with the lightest neutralino in electron-positron collisions at centre-of-mass energies up to 209 GeV. *Phys. Lett. B* **2002**, *533*, 223. https://doi.org/10.1016/S0370-2693(02)01584-8.
8. DELPHI Collaboration. Searches for supersymmetric particles in electron-positron collisions up to 208 GeV. *Eur. Phys. J. C* **2003**, *31*, 421. https://doi.org/10.1140/epjc/s2003-01355-5.

9. OPAL Collaboration. Search for nearly mass-degenerate charginos and neutralinos at LEP. *Eur. Phys. J. C* **2003**, *29*, 479. https://doi.org/10.1140/epjc/s2003-01237-x.
10. Kraml, S.; et al. SModelS: a tool for interpreting simplified-model results from the LHC. *Eur. Phys. J. C* **2014**, *74*, 2868. https://doi.org/10.1140/epjc/s10052-014-2868-5.
11. Alguero, G.; et al. SModelS v2.0: towards accurate theory predictions. *Eur. Phys. J. C* **2022**, *82*, 1. https://doi.org/10.1140/epjc/s10052-021-09931-3.
12. Drees, M.; Dreiner, H.; Schmeier, D.; Tattersall, J.; Kim, J.S. CheckMATE: Confronting your favourite new physics model with LHC data, 2013, [arXiv:hep-ph/1312.7591].
13. Drees, M.; et al. CheckMATE 2: From the model to the limit. *Comput. Phys. Commun.* **2018**, *222*, 65. https://doi.org/10.1016/j.cpc.2017.08.021.
14. Dainese, A.; et al. Physics at the HL-LHC, and Perspectives for the HE-LHC. Technical Report CERN-2019-007, CERN, 2019. https://doi.org/10.23731/CYRM-2019-007.